J Therm Anal Calorim (2009) 97:231–237
DOI 10.1007/s10973-009-0261-7

Preparation and characterization of alumina-doped powders for the design of multi-phasic nano-microcomposites

V. Naglieri · P. Palmero · L. Montanaro

ICTAC2008 Conference

Abstract The composite powders 90 vol.% Al_2O_3–5 vol.% YAG–5 vol.% ZrO_2 were produced by doping commercial alumina powders with zirconium and yttrium chloride aqueous solutions. Both a nanocrystalline transition alumina and a pure α-phase powder were used as starting materials. The obtained materials were characterized by DTA-TG, XRD and dilatometric analyses and compared to the respective biphasic systems developed by the same procedure. Pressureless sintering at 1500 °C for 3 h was able to consolidate the doped powders in fully dense bodies, characterized by a very fine and homogeneous dispersion of the second phases into the micronic alumina matrix.

Keywords Alumina-based nanocomposite · Cubic zirconia · Multi-phase composites · YAG

Abbreviations

T-A	α-alumina (TM-DAR Taimicron)
N-A	Nanocrystalline transition alumina (NanoTek®)
T-AZ5	95 vol.% Al_2O_3–5 vol.% YAG obtained from T-A doping
T-AY5	95 vol.% Al_2O_3–5 vol.% YAG obtained from T-A doping
N-AY5	95 vol.% Al_2O_3–5 vol.% YAG obtained from N-A doping
N-AY10	90 vol.% Al_2O_3–10 vol.% YAG obtained from N-A doping
N-AY20	80 vol.% Al_2O_3–20 vol.% YAG obtained from N-A doping
T-AYZ	90 vol.% Al_2O_3–5 vol.% YAG–5 vol.% ZrO_2 obtained from T-A doping
N-AYZ	90 vol.% Al_2O_3–5 vol.% YAG–5 vol.% ZrO_2 obtained from N-A doping

V. Naglieri (✉) · P. Palmero · L. Montanaro
Department of Material Science and Chemical Engineering – Politecnico di Torino, INSTM Research Unit – LINCE Lab., Corso Duca degli Abruzzi 24, 10129 Torino, Italy
e-mail: valentina.naglieri@polito.it

Introduction

In many industrial applications, components are required to work in extremely harsh conditions, particularly at very high-temperatures for long times. For these applications, new ceramic matrix composites have been designed, in which nano-sized reinforcing particles, located at inter or intra-granular positions, could improve mechanical performances as well as strongly reduce creep rate [1, 2]. Many attempts are in progress to develop biphasic systems, for instance based on micro-grained alumina matrices reinforced by nano-dispersions of various oxide or non-oxide materials [3], such as ZrO_2 [4], $Y_3Al_5O_{12}$ (YAG) [5, 6], SiC [7]. Ceramic biphasic nanocomposites can be elaborated by using various processing routes starting from nanopowder mixing [4, 7, 8] or by nanocomposite powders obtained by coprecipitation of complex compositions [6, 9]. Recently, an innovative procedure, named powder–alkoxide mixture, starting from a commercial α-alumina powder, and using a zirconium alkoxide and yttrium methoxyethoxide as doping agents, was exploited to prepare alumina–zirconia and alumina–YAG micro-nano-composite materials, respectively [3, 10]. A composite materials containing $MgAl_2O_4$–ZrO_2 was also developed by sol–gel coating of a sub-micronic spinel powder, using zirconium *n*-propoxide as zirconia precursor [11]. Few studies report about the elaboration of alumina-based tri-phasic composites. One of the most investigated systems is

the alumina–mullite–zirconia one, obtained by reaction sintering [12–15], and recently produced also at the nano-scale by the powder–alkoxide mixture route [16]. Nano-sized SiC was dispersed into ZrO_2–Al_2O_3 composites by hot-pressing a powder mixture, in view of investigating the role of SiC grains in limiting the grain growth in the ZrO_2–Al_2O_3 system by pinning effect [17]. Three-phased composites containing Al_2O_3–ZrO_2–YAG have been already obtained by rapid solidification of a melt [18, 19].

This paper deals with the preparation of alumina-based nanocomposites reinforced by two-second phases, namely ZrO_2 and YAG, in the following composition: 90 vol.% Al_2O_3–5 vol.% YAG–5 vol.% ZrO_2. These materials were obtained by doping both a nanocrystalline transition and a pure α-phased commercial alumina powders by using aqueous solutions of the inorganic metal salts as precursors of the final oxides. The adopted procedure was successfully exploited in recent papers to prepare the respective biphased systems, namely 95 vol.% Al_2O_3–5 vol.% ZrO_2 [21, 22] and 95 vol.% Al_2O_3–5 vol.% YAG [20–22], which were used as reference materials in this work.

Experimental

Two commercial alumina nanopowders were used as composite matrix: a α-alumina powder (Taimei, TM-DAR TAIMICRON, labelled as T-A), characterized by a mean particle size of 350 nm [23], and a nano-crystalline transition alumina (NanoTek®, supplied by Nanophase Technologies, USA, labelled as N-A). This latter has an average crystallite size of about 47 nm [24] and it transforms into the α-phase at about 1300 °C.

Both powders were firstly dispersed in distilled water by ball milling for 3 h (powder/spheres mass ratio of 1:10, alpha-alumina balls of 2 mm in diameter), and then added with the aqueous solutions of the inorganic metal salts, following a procedure already described in literature [20]. $ZrCl_4$ and $YCl_3{\cdot}6H_2O$ (0.3 M) aqueous solutions were used as source to yield ZrO_2 and YAG, respectively. In the case of zirconium chloride aqueous solution, the pH is less than 1, so a proper amount of tribasic ammonium citrate was added (molar ratio ammonium citrate:$ZrCl_4$ equal to 2:1), in order to reach a pH of 4.5 and avoid corrosion problems of the spray-drier steel parts. In fact, after homogenisation under stirring for 1 hour, the doped suspensions were diluted down to 4 wt% and dried by atomisation (Mini Spray Dried Büchi B-290) to avoid segregation of the added salts.

Biphasic systems, with composition 95 vol.% Al_2O_3–5 vol.% ZrO_2, named T-AZ5, and 95 vol.% Al_2O_3–5 vol.% YAG, labelled T-AY5 and N-AY5 [20–22], were used as reference materials in this work. In the case of triphasic composites, 90 vol.% Al_2O_3–5 vol.% YAG–5 vol.% ZrO_2, named N-AYZ or T-AYZ respectively, many attempts were performed to set-up the order of the solutions addition, the intermediate thermal treatments as well as the global amount of the added salts. In fact, some experimental problems were observed in controlling phase development and purity due to the fact that YAG is yielded by solid-state reaction of yttrium salt on the alumina powder surface at relatively high temperature (starting from 1300 °C), but yttrium ions are also solid-state soluble into the zirconia lattice giving rise to a metastabilization of tetragonal or even cubic phases. As described in the followings, to overpass such a problem, $YCl_3{\cdot}6H_2O$ content was increased from the stoichiometric content just needed to yield 5 vol.% YAG, to the amount also required to fully stabilize 5 vol.% ZrO_2 in the cubic state ($Zr_{0.72}Y_{0.28}O_{1.862}$). For a better understanding of the role of the yttrium content on reaction path and products yielding, two bi-phase systems with composition 90 vol.% Al_2O_3–10 vol.% YAG (N-AY10) and 80 vol.% Al_2O_3–20 vol.% YAG (N-AY20) were also prepared, by doping N-A with 18.5 and 39.1 wt% of $YCl_3{\cdot}6H_2O$, respectively, by following the above described procedure.

The thermal behaviour of the as-dried, pure and doped powders was investigated by simultaneous DTA-TG (Netzsch 409 STA) analyses (performed on about 0.150 g of powdered samples, in static air, using alpha-alumina crucibles, heating rate of 10 °C/min).

The spray-dried granules were thermal treated at different temperatures and phase evolution was followed by X-Ray diffraction (XRD, Philips PW 1710, Cu anticathode, λ_{cu} 1.54060 Å, 2θ range 5–70°).

Pre-treated powders were then uniaxially pressed in bars at about 300 MPa and their sintering behaviour was followed by absolute dilatometry (Netzsch 402E). The density of sintered bodies was evaluated by exploiting green density, final mass measurements and shrinkage data. The microstructure of the composite materials was observed by using SEM (Hitachi S2300) microscopy.

Results and discussions

Set-up of the doping procedure

Both as-received N-A and T-A powders are characterized by a significant agglomeration so that a dispersion step is necessary before doping, to promote the homogeneous distribution of second phases into the alumina matrix. For both powders, 3 h of ball milling were enough to achieve highly dispersed suspensions whose agglomerate size distributions were below 1 μm [21].

The first attempt was performed by a double-step procedure. After dispersion, the alumina powders were firstly

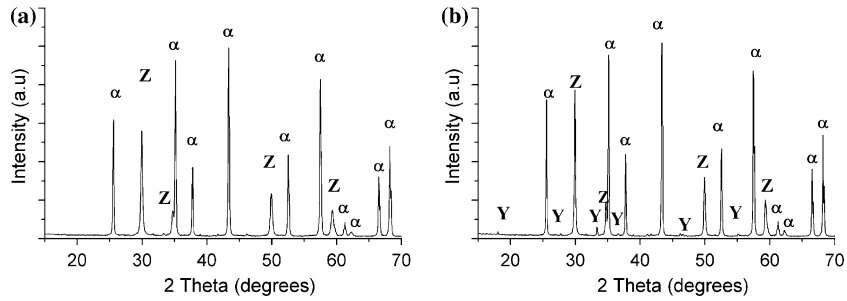

Fig. 1 XRD patterns of T-AYZ powders, treated at 1300 °C (**a**) and 1400 °C (**b**) for 30 min, (α = α-alumina, Z = c-Zirconia, Y = YAG)

added with the $ZrCl_4$ aqueous solution, spray-dried and then calcined at 600 °C for 1 h, since at this temperature tetragonal zirconia was clearly detected in the T-AZ5 composite by XRD [21]. After that, the powder was re-dispersed in the $YCl_3{\cdot}6H_2O$ aqueous solution, atomised and treated at high temperatures, at which yttrium aluminates, precisely YAG and orthorhombic perovskite $YAlO_3$, are yielded, as stated on the ground of the experiences performed on both T- and N-AY5 materials [21]. However, in the case of the triphasic system, after calcination at 1300° and at 1400 °C for 30 min (Fig. 1a, b), YAG was detectable just in traces, since most of the yttrium was used to yield the cubic phase $Zr_{0.72}Y_{0.28}O_{1.862}$ (ICDD n° 77-2112).

Another attempt was then performed by following the above procedure, modifying the pre-calcination temperature from 600 °C to 1000 °C (for 1 h) in order to induce a better crystallization of zirconia before yttrium addition, and consequently trying to reduce yttrium diffusion in its lattice. XRD results revealed that, however, also this test was unsuccessful.

Finally, the amount of yttrium was increased in order to fully stabilize as cubic phase the 5 vol.% ZrO_2 present in the mixture, on the ground of the phase diagram [25, 26], as well as to assure an excess of yttrium able to yield the expected 5 vol.% YAG.

Since an yttrium percentage of about 15 mol.% is needed for the cubic phase stabilization [25], a total amount of 15.12 wt% of $YCl_3{\cdot}6H_2O$ (referred to the alumina content) was added following two different procedures; in one case, the yttrium solution was added to the alumina powders already doped with the zirconium salt solution, spray-dried and pre-treated at 600 °C for 1 h (that is the previously stated double-step process); in the second one (which will be referred as the single-step procedure), the two doping solutions were added to the dispersed alumina powders at the same time, and then the slurries were atomised and calcined. Independently from the procedure, in both cases, after calcination at 1400 °C for 30 min, α-alumina was detected near cubic ZrO_2 and well-crystallised YAG (Fig. 2). Since the final results are fully equivalent, it was decided to continue the experimentation by exploiting the simplest way, that is the single-step process.

Thermal behaviour of pure and doped samples by DTA-TG analyses

T-A doped samples were submitted to DTA-TG analyses for investigating the crystallization temperature range of the second phases. However, probably due to the low volume percentage (5%) of the added second phases, it was not possible to detect appreciable calorimetric signals imputable to ZrO_2 and/or YAG crystallization. In contrast, DTA-TG data collected on N-A, N-AY and of N-AZY materials allowed to recognize the effect of the dopants on the θ to α-Al_2O_3 crystallization temperature.

Pure N-A presents a sharp exothermal signal at about 1180 °C, which could be attributed to the crystallization of the α-phase from transition alumina, as stated by the literature [27] and confirmed by XRD analyses performed on the powder calcined around this temperature range. The thermal evolution of N-A is associated to a limited mass loss of about 1.3 wt%, as evidenced by the TG curve. N-AY presents a higher mass loss (about 5 wt%), to be mostly imputed to residual chlorides decomposition, and a DTA exothermal peak at about 1265 °C. Finally, N-AYZ

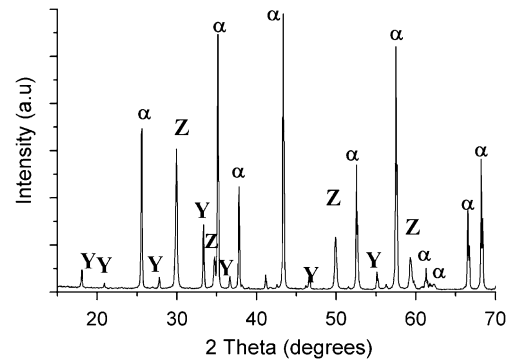

Fig. 2 XRD patterns of T-AYZ powder calcined at 1400 °C for 30 min, prepared by a single-step procedure (α = α-alumina, Z = c-Zirconia, Y = YAG)

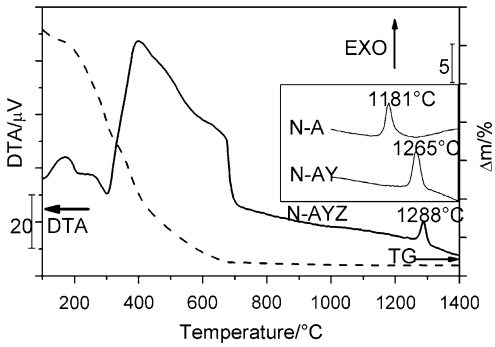

Fig. 3 DTA (*solid line*)–TG (*dashed line*) curves of N-AYZ. In the insert, DTA curves of N-AY and N-A samples in the 1000–1400 °C temperature range

was characterized by a total mass loss of about 33 wt%, almost completely recorded in the 100–700 °C temperature range, imputable to both ammonium citrate and chlorides thermal decomposition, while α-Al_2O_3 crystallization occurred at about 1288 °C. Thus, a significant effect of dopants in delaying α-alumina crystallization was clearly stated, in a good agreement with literature data [27]. In Fig. 3, DTA (solid line)–TG (dashed line) curves of N-AYZ are reported; for a sake of comparison, the DTA curves of N-AY and N-A samples in the 1000–1400 °C temperature range are also inserted.

Phase evolution by XRD analysis

Considering the phase evolution as a function of the treatment temperature, low-temperature phenomena, mainly involving zirconia crystallization, can be clearly distinguished from the high-temperature ones, such as the solid state reactions leading to yttrium aluminates formation. At low temperature, zirconia diffraction peaks can be detected starting from calcination at 400 °C, as already observed in T-AZ5 materials. In Fig. 4a, DRX patterns collected on T-AYZ are reported, showing that only α-Al_2O_3 and cubic ZrO_2 were detected up to 1000 °C. From the XRD patterns of the powders calcined at 400 °C, the influence of yttrium in zirconia crystallization can be appreciated. In Fig. 4b, the main peak of the tetragonal ZrO_2 in T-AZ5 and of the cubic phase in T-AYZ are compared: the peak related to cubic ZrO_2 is broader and weaker, supporting the slight retard in primary crystallization of zirconia due to yttrium, as already stated in literature [28].

The yttrium aluminates phase evolution into the multiphase composites is shown in Fig. 5 where XRD patterns collected on N-AY5 (a) and N-AYZ (b) powders calcined in the 1300–1500 °C temperature range can be compared. After calcination at 1300 °C for 30 min, YAG and orthorhombic perovskite $YAlO_3$ (YAP, labelled as P) were detected in both materials (curves I). However, after calcination at higher temperatures, the undesired second phase progressively disappeared (see curves II and III of Fig. 5). A similar behaviour was observed in T-doped samples (Fig. 6). In fact, YAP was once again detected in T-AY5 calcined at 1300 °C (curve I of Fig. 6a), but its amount decreased while increasing the calcination temperature (curves II and III of Fig. 6a). Pure YAG crystallized at 1300 °C in T-AYZ material, and it remained the only phase detected near α-Al_2O_3 and cubic ZrO_2 up to 1500 °C for 30 min.

In order to better investigate the reaction mechanisms as well as to understand the appearance of the intermediate perovskite phase, having a different stoichiometry with respect to the expected garnet, a deeper investigation on the role of yttrium content on the crystallization path of both α-Al_2O_3 and yttrium aluminates was therefore performed.

For a sake of simplicity, such study was performed on biphasic alumina-YAG systems based on N-A powders, since detectable amounts of perovskite phase were clearly observed also in the related triphasic material. Being the yttrium amount needed to develop the triphasic system supplied by the addition of about 15 wt% $YCl_3{\cdot}6H_2O$ referred to the alumina content, composites N-AY ranging from 5 vol.% YAG (about 9 wt% $YCl_3{\cdot}6H_2O$) to 20 vol. % YAG (about 39 wt% $YCl_3{\cdot}6H_2O$) were prepared.

From XRD analyses, a strong influence of the yttrium content on both crystallization temperature of yttrium aluminates and their transformation temperature into YAG phase, as well as on α-phase appearance from transition

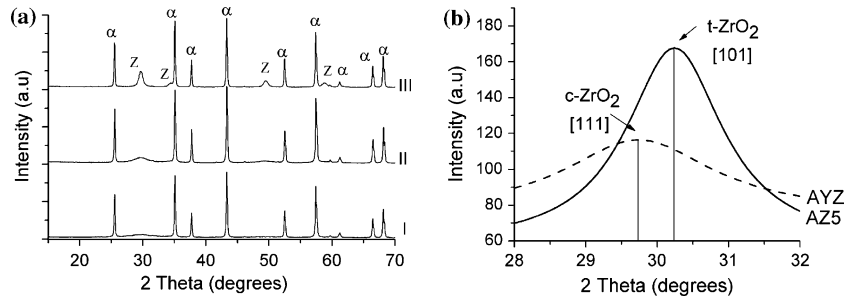

Fig. 4 **a** XRD patterns of T-AYZ powder calcined at 400 °C (I) and 600 °C (II) for 60 min and at 1000 °C for 30 min (III); **b** XRD patterns in the 28–32 °2θ range of T-AYZ (*dashed line*) and AZ5 (*solid line*) powders calcined at 400 °C for 1 h (α = α-alumina, Z = c-Zirconia)

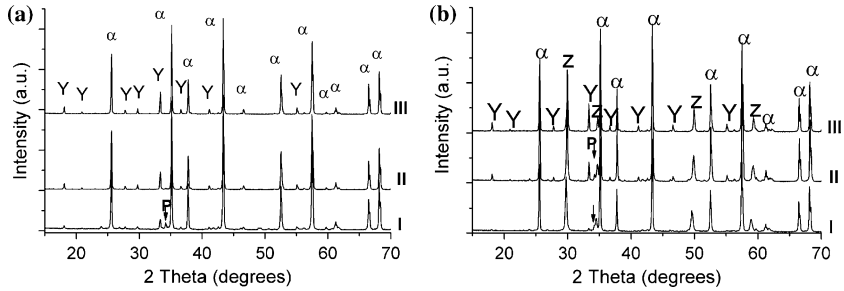

Fig. 5 XRD patterns of N-AY5 (**a**) and N-AZY (**b**) calcined at 1300 °C (curves I), 1400 °C (curves II), and 1500 °C (curves III) for 30 min (α = α-alumina, Z = c-Zirconia, Y = YAG, P = YAP)

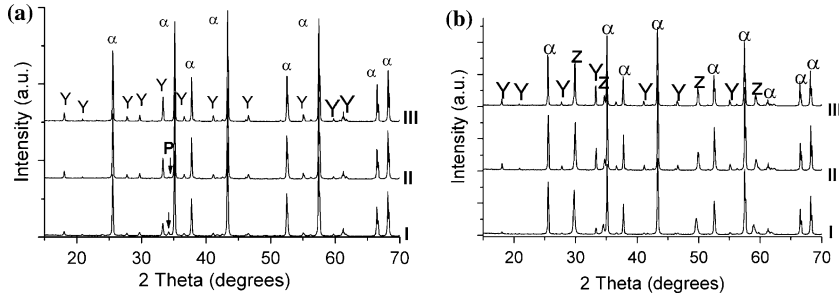

Fig. 6 XRD patterns of T-AY5 (**a**) and T-AZY (**b**) calcined at 1300 °C (curves I), 1400 °C (curves II), and 1500 °C (curves III) for 30 min (α = α-alumina, Z = c-Zirconia, Y = YAG, P = YAP)

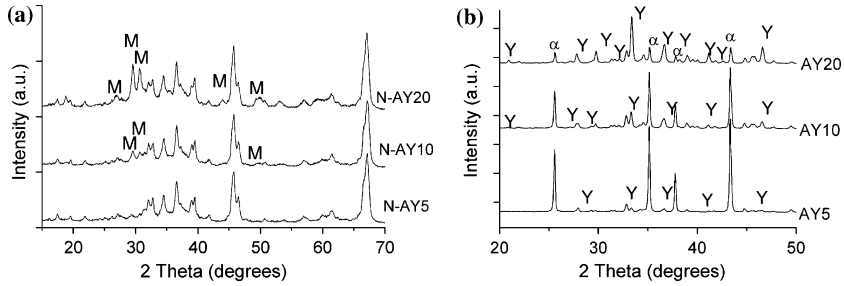

Fig. 7 XRD patterns of N-AY5, N-AY10 and N-AY20 calcined at 900 °C (**a**) and 1200 °C (**b**) for 30 min (α = α-alumina, Y = YAG, M = YAM)

aluminas was stated. In fact, in N-AY5 treated at 900 °C for 30 min (Fig. 7a), only transition aluminas can be detected. In contrast, in N-AY10 traces of the monoclinic $Y_4Al_2O_9$ (YAM, labelled as M) were detected and the same phase, but better crystallized, was present in N-AY20.

Therefore, the higher the yttrium content, the lower the temperature of crystalline yttrium aluminates appearance. In the case of the yttrium-richer materials, the first product yielded is also the yttrium-richest aluminate in the related phase diagram.

From some microscopic investigations exploiting high-resolution means, still in progress [29], an amorphous layer rich in yttrium was observed on the surface of the transition alumina particles and aluminates seem to be yielded by a progressive yttrium diffusion toward the bulk of the alumina grains. As a consequence, the appearance of yttrium-richer phases should be considered as an intermediate step of the overall reaction, which will lead to a homogeneous system, finally yielding YAG, thus respecting the stoichiometry imposed during the doping phase. Improving the treatment temperature at 1150 °C, N-AY5 still contained only transition aluminas, confirming the delaying in crystallization for the poorest yttrium mixture, while in N-AY10 YAG and traces of the metastable, hexagonal phase (h-$YAlO_3$) were identified and the same phases, but better crystallized, were detected in N-AY20. Therefore, increasing the calcination temperature from 900 °C to 1150 °C, thanks to the higher diffusion rates, monoclinic phase disappeared, replaced by another intermediate phase less rich in yttrium (h-$YAlO_3$) near the expected YAG composition.

After treatment at 1200 °C for 30 min (Fig. 7b), YAG and the hexagonal phase were also detected in the N-AY5, likewise the other composites. In addition, comparing the

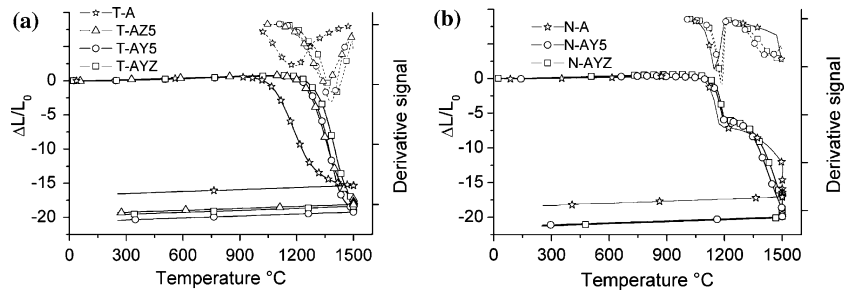

Fig. 8 Dilatometric and derivative curves of pure and doped **a** T-samples and **b** N-samples

three patterns, a delaying of α-alumina crystallization due to the increase of the yttrium content was observed. At 1300 °C for 30 min, YAG and the stable perovskite (having the same stoichiometry as h-$YAlO_3$) were still detectable in N-AY5 and N-AY10, whereas already pure YAG was observed near α-Al_2O_3 in N-AY20. All the materials yielded a completely biphasic system after calcination at 1500 °C. Yttrium aluminates in N/T-AYZ were not detected up to 1200 °C, showing a delaying in crystallization of these phases probably due to zirconia presence. In contrast at 1300 °C, YAG and perovskite (in traces) were present similarly to N-AY5 and N-AY10, as expected on the ground of its yttrium amount.

Sintering behaviour

The triphasic powdered compacts were sintered exploiting thermal cycles already set-up on the pure powders as well as on the respective biphasic composites [20–22]. Namely, pure and doped Taimei samples were heated up to 1100 °C at 10 °C/min and then up to 1500 °C at 2 °C/min with a dwelling time of 3 h at the maximum temperature. In Fig. 8a, the dilatometric curves of T-A, T-AZ5, T-AY5 and T-AZY are compared. The four samples showed comparable green densities of about 2.1–2.3 g/cm^3; after sintering the doped materials reached almost full densification, while pure Taimei yielded a fired density of 97.2% of the theoretical value. In addition, it should be observed that both biphasic and triphasic systems show a delay of the onset sintering temperature when compared to pure alumina. Also the maximum sintering rate temperature, corresponding to the inflection point of the derivative curves shown in the same Figure, is displaced to higher values if compared to undoped Taimei, with a higher delay for the triphasic material. Similar comments can be done for pure and doped NanoTek samples (Fig. 8b), sintered under the following thermal cycle: heating rate of 10 °C/min up to 700 °C and then 1 °C/min up to 1500 °C, and a dwelling time of 3 h. A two-step sintering behaviour, typical of transition aluminas, is even presented by the doped powders, which again show a displacement of the dilatometric curve at higher values, but less significant than for doped-Taimei samples. After sintering, N-AY5 and N-AYZ reached fired densities of 99.5 and 98.8% of the theoretical value, respectively, while a lower value of 97.5% was achieved by N-A.

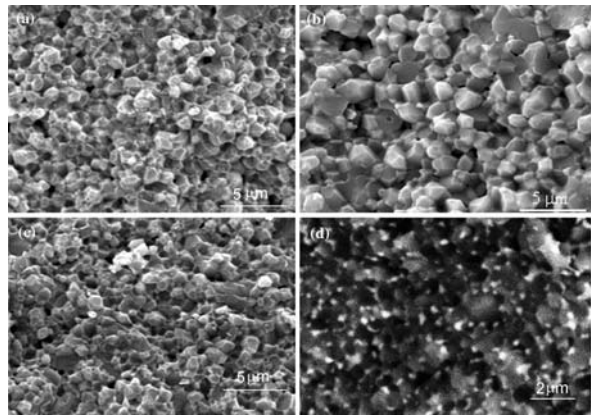

Fig. 9 SEM micrograph of N-AYZ (**a**), N-AY5 (**b**), T-AYZ (**c**) and BSE micrograph of T-AYZ (**d**) fired material

Microstructural observations

The fired tri-phasic materials yielded a fully dense and finer microstructures compared to that of bi-phasic composites, as shown in Fig. 9a and b for N-composites, and in Fig. 9c for T-AYZ. Moreover, a homogeneous distribution of the two reinforcing phases into the alumina matrix can be appreciated in the back-scattered SEM images (Fig. 9d).

Conclusions

From the above experimental results, the following conclusions can be drawn out:

– Post-doping of commercial powders is an effective way to produce micro-nanocomposite materials not only having a biphasic composition, but also made of two different reinforcement phases.

- Pure alumina-cubic zirconia–YAG composite powders have been successfully prepared by exploiting a single-step doping procedure, applied on both a transition nanocrystalline alumina or an alpha-alumina ultra fine powder;
- The single-step doping procedure was set up in order to obtain a fully stabilised cubic zirconia and YAG, without other phases in amounts detectable by XRD;
- Both composite powders are able to fully sinter, yielding microstructures in which ultra-fine second phases are homogeneously distributed into micronic alumina matrix.

References

1. Niihara K. New design concept of structural ceramics–ceramic nanocomposites. J Ceram Soc Jpn. 1991;99:974–82.
2. Sternitzke M. Review: structural ceramic nanocomposites. J Eur Ceram Soc. 1997;17:1061–82.
3. Schehl M, Diaz LA, Torrecillas R. Alumina nanocomposites from powder-alkoxide mixtures. Acta Mater. 2002;50:1125–39.
4. Sarkar D, Adak S, Mitra NK. Preparation and characterization of an Al_2O_3–ZrO_2 nanocomposite. Part I: powder synthesis and transformation behavior during fracture. Compos Part A. 2007;38:124–31.
5. Wang H, Gao L, Shen Z, Nygren M. Mechanical properties and microstructures of Al_2O_3–5 vol% YAG composites. J Eur Ceram Soc. 2001;21:779–83.
6. Palmero P, Simone A, Esnouf C, Fantozzi G, Montanaro L. Comparison among different sintering routes for preparing alumina–YAG nanocomposites. J Eur Ceram Soc. 2006;26:941–7.
7. Jeong YK, Niihara K. Microstructure and mechanical properties of pressureless sintered Al_2O_3/SiC nanocomposites. NanoStruct Mater. 1997;9:193–6.
8. Hirvonen A, Nowak R, Yamamoto Y, Sekino T, Niihara K. Fabrication, structure, mechanical and thermal properties of zirconia-based ceramic nanocomposites. J Eur Ceram Soc. 2006; 26:1497–505.
9. Li WQ, Gao L. Processing, microstructure and mechanical properties of 25 vol% YAG–Al_2O_3 nanocomposites. NanoStruct Mater. 1999;11:1073–80.
10. Torrecillas R, Schehl M, Díaz A, Menéndez JL, Moya JS. Creep behaviour of alumina/YAG nanocomposites obtained by a colloidal processing route. J Eur Ceram Soc. 2007;27:143–50.
11. Boulle A, Oudjedi Z, Guinebretière R, Soulestin B, Dauger A. Ceramic nanocomposites obtained by sol–gel coating of submicron powders. Acta Mater. 2001;49:811–6.
12. Torrecillas R, Moya JS, De Aza S, Gros H, Fantozzi G. Microstructure and mechanical properties of mullite–zirconia reaction-sintered composites. Acta Metall Mater. 1993;41:1647–52.
13. Pena P, Miranzo P, Moya JS, De Aza S. Multicomponent toughned ceramic materials obtained by reaction sintering—Part 1. ZrO_2–Al_2O_3–SiO_2–CaO system. J Mater Sci. 1985;20:2011–22.
14. Miranzo P, Pena P, Moya JS, De Aza S. Multicomponent toughned ceramic materials obtained by reaction sintering—Part 2. System ZrO_2–Al_2O_3–SiO_2–MgO. J Mater Sci. 1985;20:2702–10.
15. Melo MF, Moya JS, Pena P, De Aza S. Multicomponent toughned ceramic materials obtained by reaction sintering—Part 2. System ZrO_2–Al_2O_3–SiO_2–TiO_2. J Mater Sci. 1985;20:2711–8.
16. Torrecillas R, Schehl M, Dìaz LA. Creep behaviour of alumina–mullite–zirconia nanocomposites obtained by a colloidal processing route. J Eur Ceram Soc. 2007;27:4613–21.
17. Jang BK. Microstructure of nano SiC dispersed Al_2O_3–ZrO_2 composites. Mater Chem Phys. 2005;93:337–41.
18. Calderon-Moreno JM, Yoshimura M. Al_2O_3–$Y_3Al_5O_{12}$ (YAG)–ZrO_2 ternary composite rapidly solidified from the eutectic melt. J Eur Ceram Soc. 2005;25:1365–8.
19. Lee JH, Yoshikawa A, Fukuda T, Waku Y. Growth and characterization of Al_2O_3/$Y_3Al_5O_{12}$/ZrO_2 ternary eutectic fibers. J Cryst Growth. 2001;231:115–20.
20. Palmero P, Montanaro L. Thermal and mechanical-induced phase transformations during YAG and alumina-YAG syntheses. J Therm Anal Calorim. 2007;88:261–7.
21. Palmero P, Naglieri V, Chevalier J, Fantozzi G, Montanaro L. Alumina-based nanocomposites obtained by doping with inorganic salt solutions: application to immiscible and reactive systems. J Eur Ceram Soc. 2009;29:59–66.
22. Montanaro L, Palmero P, Fantozzi G, Chevalier J. A comparison among different processing routes towards ceramic nanocomposites development. Proc. 10th Intern. Conf. of the European Ceramic Society, Goller Verlag (DEU) Berlin, June 17–20, Vol. 1; 2007. p. 1453–60.
23. http://www.taimei-chem.co.jp.
24. http://www.nanophase.com.
25. Chen M, Hallstedt B, Gauckler LJ. Thermodynamic modeling of the ZrO_2–$YO_{1.5}$ system. Solid State Ionics. 2004;170:255–74.
26. Lakiza SM, Lopato LM. Stable and metastable phase relations in the system alumina–zirconia–yttria. J Am Ceram Soc. 1997;80: 893–902.
27. Bowen P, Carry C, Hofmann H, Legros C. Phase transformation and sintering of α-Al_2O_3—effects of powder characteristics and dopants (Mg or Y). Key Eng Mater. 1997;132:904–7.
28. Ghosh A, Upudhyaya DD, Prasad R. Primary crystallization behavior of ZrO_2–Y_2O_3 powders: in situ hot-stage XRD technique. J Am Ceram Soc. 2002;85:2399–403.
29. Palmero P, Esnouf C, Fantozzi G, Montanaro L. Microstructural and phase evolution of γ-doped alumina powders toward the elaboration of Al_2O_3–YAG nanocomposite. Proceedings of the 11th European inter-regional conference on ceramics, 3–5 September 2008, Lausanne, Switzerland, pp 123–30.